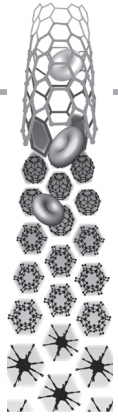

Erythrocyte membrane-cloaked polymeric nanoparticles for controlled drug loading and release

Aim: Polymeric nanoparticles (NPs) cloaked by red blood cell membrane (RBCm) confer the combined advantage of both long circulation lifetime and controlled drug release. The authors carried out studies to gain a better understanding of the drug loading, drug-release kinetics and cell-based efficacy of RBCm-cloaked NPs. **Materials & methods:** Two strategies for loading doxorubicin into the RBCm-cloaked NPs were compared: physical encapsulation and chemical conjugation. *In vitro* efficacy was examined using the acute myeloid leukemia cell line, Kasumi-1. **Results:** It was found that the chemical conjugation strategy resulted in a more sustained drug release profile, and that the RBCm cloak provided a barrier, retarding the outward diffusion of encapsulated drug molecules. It was also demonstrated that RBCm-cloaked NPs exhibit higher toxicity in comparison with free doxorubicin. **Conclusion:** These results indicate that the RBCm-cloaked NPs hold great promise to become a valuable drug-delivery platform for the treatment of various diseases such as blood cancers.

Original submitted 27 February 2012; Revised submitted 27 August 2012; Published online 14 February 2013

KEYWORDS: biomimetic nanoparticle ▪ drug delivery ▪ nanomedicine ▪ polymeric nanoparticle ▪ red blood cell membrane ▪ sustained release

Santosh Aryal[1,2], Che-Ming J Hu[1,2], Ronnie H Fang[1,2], Diana Dehaini[1], Cody Carpenter[1], Dong-Er Zhang[2] & Liangfang Zhang*[1,2]

[1]Department of NanoEngineering, University of California, San Diego, 9500 Gilman Drive, MC-0448, La Jolla, CA 92093-0448, USA
[2]Moores Cancer Center, University of California, San Diego, La Jolla, CA 92093, USA
**Author for correspondence: Tel.:+1 858 246 0999 zhang@ucsd.edu*

In recent decades, advances in engineering materials at the nanometer scale have resulted in a myriad of nanoparticle (NP)-based drug-delivery systems for clinical applications [1,2]. The unique advantages of these nanomedicines, particularly their improvement on existing therapeutic agents through altered pharmacokinetics and biodistribution profiles, hinge on their ability to circulate in the bloodstream for a prolonged period of time [3,4]. As a result, considerable research interest has focused on the search for novel materials, both natural and synthetically made, that allow NPs to bypass macrophage uptake and systemic clearance [5,6]. Meanwhile, strategies aimed at extending particle residence time *in vivo* through modifying the physicochemical properties of NPs (including size, shape, deformity and surface characteristics) have also been extensively explored [7,8].

In this regard, the authors recently developed a red blood cell membrane (RBCm)-cloaked NP drug-delivery system with the combined advantages of a long circulation lifetime (from RBCs) and controlled drug retention and release (from polymeric particles) [9]. The authors' top-down approach, based on the extrusion of polymeric particles mixed with preformed RBCm-derived vesicles, translocated the entire RBCm with preserved membrane proteins to the surface of sub 100-nm polymeric cores, resulting in NPs cloaked by the erythrocyte exterior for longer systemic circulation. This functionalization strategy enables transmembrane proteins to be anchored in their natural lipid membrane medium on nanoparticle surfaces and avoids chemical conjugation techniques that could disrupt the integrity and functionalities of these proteins.

As part of continuing efforts to further develop this cell-mimicking NP platform for advanced drug-delivery applications, the authors report formulation strategies for loading small-molecule chemotherapy drugs such as doxorubicin (DOX), a model anticancer drug, into NPs and study drug-release kinetics with an emphasis on the role played by RBCm cloaks in drug retention. Specifically, to load DOX molecules into the NP core, two distinct strategies were explored: physically encapsulating drug molecules into the polymer matrix, and chemically conjugating drug molecules to the polymer backbones. It was demonstrated that these methods result in distinct drug-loading yields and release kinetics. NPs were further formulated with the same polymer cores as RBCm-cloaked NPs, but coated with PEG rather than RBCm (PEGylated NPs). Comparison of the drug-release profiles for the two delivery systems demonstrated that the RBCm cloak provides a barrier, retarding the outward diffusion of encapsulated drug molecules, and can therefore

Future Medicine part of fsg

potentially be exploited to better control drug release. Additionally, in an attempt to examine the therapeutic potential of the RBCm-cloaked NPs, an acute myeloid leukemia (AML) Kasumi-1 cell line was chosen, and it was demonstrated that DOX-loaded RBCm-cloaked NPs exhibited higher toxicity by comparison with the same amount of free DOX.

Materials & methods

RBC ghost derivation

RBC ghosts devoid of cytoplasmic contents were prepared following previously published protocols [9,10]. Briefly, whole blood, withdrawn from male (imprinting control region)mice (6–8 weeks old; Charles River Laboratories, MA, USA) through cardiac puncture with a syringe containing a drop of heparin solution (Cole-Parmer, IL, USA), was centrifuged (800 × *g* for 5 min at 4°C) to remove serum and buffy coat. The packed RBCs were washed in ice-cold 1× phosphate-buffered solution (PBS), treated by hypotonic medium for hemolysis, and then suspended in 0.25× PBS in an ice bath for 20 min. The hemoglobin was removed by centrifuging the suspension at 800 × *g* for 5 min. RBC ghosts in the form of a pink pellet were collected.

Preparation of RBCm-derived vesicles

The collected RBC ghosts were sonicated in a capped glass vial for 5 min using a FS30D bath sonicator (Fisher Scientific, CA, USA) at a frequency of 42 kHz and power of 100 W. The resulting vesicles were subsequently extruded repeatedly through 400-nm and then 200-nm polycarbonate porous membranes using an Avanti mini extruder (Avanti Polar Lipids, AL, USA). After each extrusion, the size of the RBCm-derived vesicles was monitored using dynamic light scattering (Nano-ZS, model ZEN3600; Malvern Instruments, Worcestershire, UK).

Ring-opening polymerization of L-lactide

DOX–poly(lactide acid) (PLA) conjugates were synthesized based on a previously published protocol [11,12]. Briefly, ring-opening polymerization of L-lactide (Sigma-Aldrich, MO, USA) was catalyzed by an alkoxy complex (β-diiminate [BDI])$ZnN(SiMe_3)_2$ in a glovebox filled with argon at room temperature. (BDI) $ZnN(SiMe_3)_2$ (6.4 mg, 0.01 mmol) and DOX (Jinan Wedo Co. Ltd, Shandong Province, China; 5.4 mg, 0.01 mmol) were first mixed in anhydrous tetrahydrofuran (0.5 ml). L-lactide (101 mg, 0.7 mmol) dissolved in 2 ml of anhydrous tetrahydrofuran was then added dropwise to the reaction mixture. After the L-lactide was completely consumed as indicated by proton nuclear magnetic resonance spectroscopy (Varian Mercury 400 MHz spectrometer; International Equipment Trading Ltd, IL, USA), the crude product was precipitated in cold diethyl ether and purified by multiple dissolution–precipitation cycles. The conjugation was confirmed by proton nuclear magnetic resonance spectroscopy and conjugates had a molecular weight (MW) of approximately 10,000 g/mol determined by gel permeation chromatography (Viscotek, TX, USA).

Preparation of NP core & loading of DOX

The DOX–PLA conjugate was first dissolved in acetonitrile to form 1 mg/ml solution. A total of 1 ml of such solution was added dropwise to 3 ml of water. The mixture was then stirred in open air for 2 h, allowing the acetonitrile to evaporate. The resulting solution of NP cores was washed using Amicon Ultra-4 Centrifugal Filters (Millipore, CA, USA; 10 kDa cut-off) to completely remove organic solvent residues. The particles were then re-suspended in 1 ml distilled water. To physically encapsulate DOX, 1 mg poly(lactic-*co*-glycolic acid [PLGA]; 0.67 dl/g, carboxy-terminated, LACTEL Absorbable Polymers, CA, USA) was first dissolved into 1 ml acetonitrile, followed by the addition of DOX predissolved in 25 µl dimethyl sulfoxide. Similar procedures as described above were followed to generate suspensions containing NP cores.

Fusion of RBCm-derived vesicles with NP cores

To fuse the RBCm-derived vesicles with the aforementioned NP cores, a suspension containing 1 mg of NP cores was first mixed with RBCm-derived vesicles prepared from 1 ml of whole blood. The mixture was then extruded 11 times through a 100-nm polycarbonate porous membrane with an Avanti mini extruder. To fully coat 1 mg of NP cores, an excess of blood was used to compensate for the membrane loss during RBC ghost derivation and extrusion [9].

Preparation of PEGylated NPs

The DOX–PLA conjugate and PLA-PEG-COOH (MW = 10 kDa, polydispersity index = 1.12; PEG = 3.5 kDa, PLA = 6.5 kDa) [13] at a weight ratio of 1:1 were first dissolved in acetonitrile at a concentration of 1 mg/ml, followed by the same procedures as described above to produce

NP suspensions. To physically encapsulate DOX into PEGylated NPs, 1 mg PLGA (0.67 dl/g, MW = 40 kDa, carboxy-terminated, LACTEL Absorbable Polymers) was first dissolved into 1 ml acetonitrile, followed by the addition of 100 µg DOX dissolved in 25 µl dimethyl sulfoxide. The procedures described above were used to produce NP suspensions.

NP stability studies

NP stability in PBS was assessed by monitoring particle size using dynamic light scattering. Specifically, 500 µg of the NPs were suspended in 1 ml 1× PBS and the sizes were measured in triplicate at room temperature every 24 h over a period of 1 week. Between measurements, samples were incubated at 37°C with gentle shaking. NP serum stability was evaluated by monitoring the UV-absorbance at a wavelength of 560 nm. Specifically, NPs were first concentrated to 2 mg/ml in PBS, followed by the addition of 2× fetal bovine serum (Hyclone; Thermo Scientific, CA, USA) of equal volume. The absorbance was measured using an Infinite M200 multiplate reader (Tecan Group Ltd, CA, USA) at 37°C approximately every 1 min over a period of 2 h. The morphology and particle size were further characterized using scanning electron microscopy (SEM). Samples for SEM were prepared by dropping 5 µl of the NP solution onto a polished silicon wafer. After drying the droplet at room temperature overnight, the sample was coated with chromium and then imaged using SEM.

Measurement of drug-loading yield & releases

The concentration of DOX in solution was determined by measuring fluorescence intensities at 580 nm with an excitation wavelength of 480 nm. To determine the DOX-loading yield of the NPs, the above fluorescence measurement was carried out after incubating 100 µl NP solution with 100 µl 0.1 M HCl in acetonitrile for 24 h. All fluorescent measurements were performed under the same conditions with 0.1 M HCl. To plot DOX release profiles, 200 µl NP solution (1 mg/ml) was loaded into a Slide-A-Lyzer MINI dialysis microtube (Pierce, IL, USA; MW cutoff: 3.5 kDa) and then dialyzed against 2 l of PBS (pH = 7.4) at 37°C. PBS buffer was changed every 12 h throughout the whole dialysis process. At each predetermined time point, NP solutions from three mini dialysis units were collected and DOX concentration was measured. Note that the hydrophobic DOX–PLA conjugates are unlikely to be released from the hydrophobic particles to aqueous solutions, as that is an energetically unfavorable process. It is expected that only drug molecules that have detached from the polymer chains will be released.

Cell viability assay

Cytotoxicity of free DOX and DOX-loaded NPs was assessed against Kasumi-1 cell line established from the peripheral blood of an AML patient using 3-(4,5-dimethylthiazol-2-yl)-2,5-diphenyltetrazolium bromide assay (Promega Corporation, WI, USA). Cells were first seeded (~5 × 10^3 per well) in 96-well plates and incubated for 24 h. After the addition of free DOX or DOX-loaded NPs, the cells were incubated for an additional 72 h. Cell viability was then determined by using 3-(4,5-dimethylthiazol-2-yl)-2,5-diphenyltetrazolium bromide assay following a protocol provided by the manufacturer.

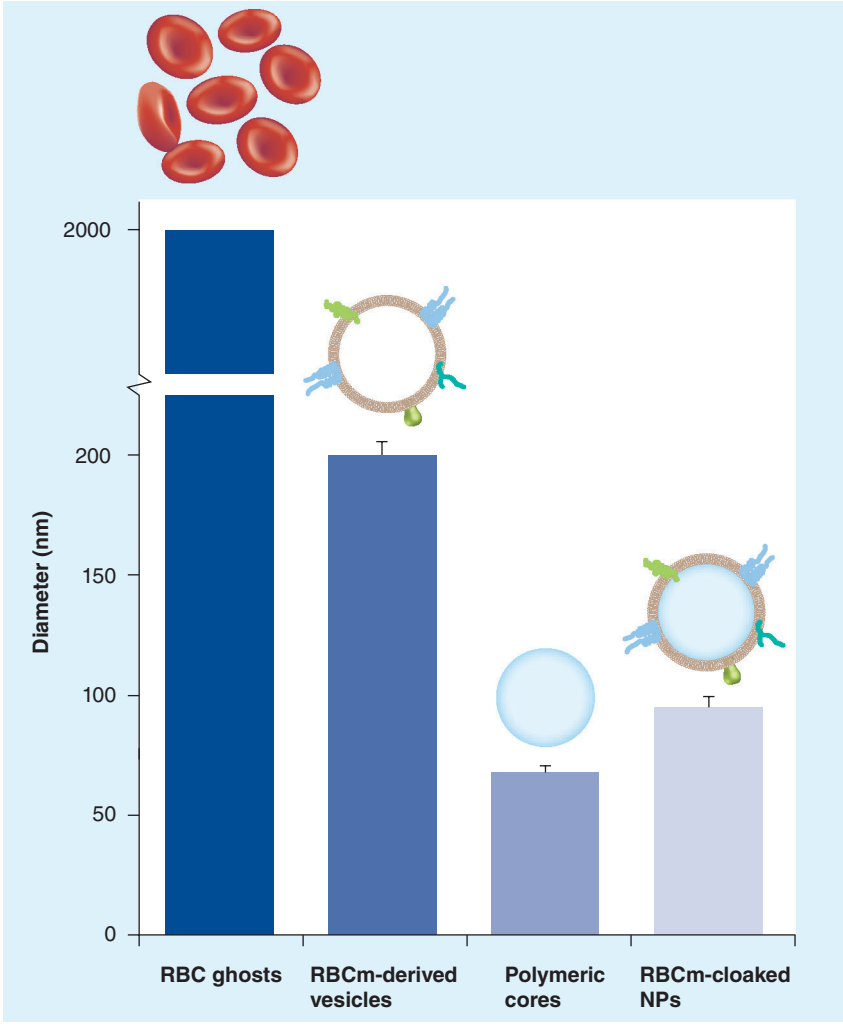

Figure 1. Building materials and the preparation process of red blood cell membrane-cloaked nanoparticles. The hydrodynamic sizes of RBC ghosts, RBCm-derived vesicles, polymeric cores and RBCm-cloaked NPs were measured using dynamic light scattering.
NP: Nanoparticle; RBC: Red blood cell; RBCm: Red blood cell membrane.

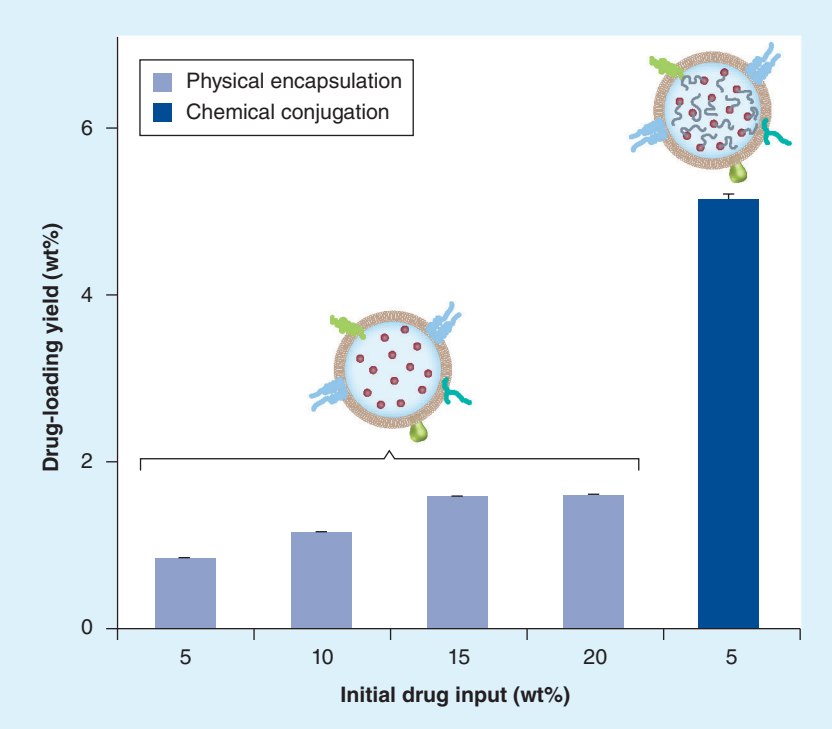

Figure 2. Doxorubicin loading yields in the red blood cell membrane-cloaked nanoparticles at various initial drug inputs. Drug molecules were loaded into the nanoparticles through two distinct loading mechanisms: physical encapsulation and chemical conjugation.

Results & discussion

Preparation of RBCm-cloaked NPs

The preparation process of RBCm-cloaked NPs was based on a previously published protocol and is schematically illustrated in Figure 1 [9]. Briefly, purified RBCs first underwent membrane rupture in a hypotonic environment to remove their intracellular contents. Next, the emptied RBCs (~2 µm in diameter) were washed and extruded through 200-nm porous membranes to create RBCm-derived vesicles (~200 nm in diameter). Meanwhile, polymeric cores (~70 nm in diameter), such as those made from PLA or PLGA, were prepared by using a solvent displacement method. The resulting polymeric cores were subsequently mixed with RBCm-derived vesicles and the mixture was physically extruded through 100-nm pores, where the two components fused under the mechanical force and formed RBCm-cloaked NPs (~90 nm in diameter).

Loading of DOX into RBCm-cloaked NPs

In this study, two distinct methods to load DOX as a model drug into the RBCm-cloaked NPs were examined: physical encapsulation and chemical conjugation. Physical encapsulation is achieved by first mixing DOX and the polymers in acetonitrile, followed by precipitation into water. In this case, the drug-loading yield can be varied through different formulation parameters. For example, when varying initial DOX to PLGA weight ratio from 5 to 20%, the loading yield increases from 0.9 to 1.8% (Figure 2).

Alternatively, DOX molecules can be loaded into NP cores by covalently conjugating drug molecules to polymer backbones. Intuitively, DOX molecules can be directly conjugated to carboxyl-terminated PLA chains through hydroxyl groups; however, this approach causes heterogeneities for polymer–drug conjugates, owing largely to the polydispersity of the polymer chains, the lack of control over the regio- and chemo-selective conjugation of the DOX molecules containing multiple hydroxyl groups, and the lack of control over the conjugation efficiency. Therefore, an alternative approach was adopted, where the hydroxyl groups of the DOX, in the presence of L-lactide monomer and using $(BDI)ZnN(SiMe_3)_2$ as a catalyst, were utilized to initiate the ring-opening polymerization and led to the formation of PLA–DOX conjugates [11,12]. In this approach, as the polymerization reaction is initiated by the drug molecule itself, a conjugation efficiency of near 100% can be achieved. In addition, the metal amido catalyst $(BDI)ZnN(SiMe_3)_2$ preferentially allows for PLA propagation at C_{14}-OH position of DOX, instead of its more sterically hindered C_4'- and C_9-OH positions. After the reaction was terminated, products were purified through repeated dissolution–precipitation cycles and then characterized using ^{1}H–NMR spectroscopy. Proton resonance peaks corresponding to both DOX molecules and PLA backbones are present, including the aromatic protons of DOX between δ = 7.5 and 8.0 ppm, protons of -CH_3 group of PLA at δ = 1.5 ppm, and -CH group of PLA at δ = 5.2 ppm, hence confirming the formation of PLA–DOX conjugates [11]. In contrast to physical encapsulation, where the drug-loading yield primarily depends on formulation parameters, in chemical conjugation, the drug-loading yield is dictated by polymer chain length, which is in turn determined by polymerization conditions such as initiator (DOX)-to-monomer ratio. For example, the PLA–DOX conjugates synthesized in this study were found to have a molecular weight of 10 kDa and a narrow polydispersity index of 1.16, corresponding to an approximately 5% loading yield of DOX after the conjugates were formulated into the NPs (Figure 2).

In vitro stability of DOX-loaded RBCm-cloaked NPs

Next, the stability of DOX-loaded RBCm-cloaked NPs in physiologically relevant buffer solutions was studied. In PBS, NP stability is monitored by measuring NP sizes at different time points, as unstable particles tend to aggregate and their sizes increase. In this study (Figure 3A), NPs loaded with DOX molecules by using both physical encapsulation and chemical conjugation showed similar initial diameters of approximately 90 nm; without significant size increase over the duration of 1 week. Similarly, only a slight change in the polydispersity index of the NPs was observed over the same time period, indicating a high stability of DOX-loaded RBCm-cloaked NPs in PBS. NP stability was further examined in serum by monitoring UV absorbance at 560 nm, a characteristic wavelength reflecting the extent of particle aggregation [14,15]. RBCm-cloaked NPs, loaded with DOX molecules by either physical encapsulation or chemical conjugation, showed a near constant absorbance at 560 nm over a time period of 2 h (Figure 3B), suggesting that the NPs are highly stable in 100% fetal bovine serum. The morphological measurements of these RBCm-cloaked NPs by SEM showed spherical structures with an average size of approximately 75 nm (Figure 3C). By contrast, absorbance of bare polymeric cores made from PLGA or PLA–DOX conjugates without RBCm cloaks immediately increased upon addition into fetal bovine serum, therefore the authors were unable to monitor their long-term stability in either PBS or serum. The results of this study showed that the RBCm cloak played a significant role in stabilizing NPs in both buffer solutions and serum. From a practical perspective, the fast aggregation of uncoated polymeric particles in buffer solutions provided a means of selective precipitation and removal of uncoated particles from RBCm-cloaked NPs after their preparation.

Release kinetics of DOX from RBCm-cloaked NPs

Following the formulation of stable DOX-loaded RBCm-cloaked NPs, their DOX release kinetics were investigated (Figure 4). The authors first examined how different drug-loading mechanisms would affect DOX releases from RBCm-cloaked NPs. The results demonstrated that, when DOX molecules were physically encapsulated into the polymer matrix, the drug-release rate was significantly faster, as 20% of DOX molecules were released within the first 2 h from the RBCm-cloaked NPs. By contrast,

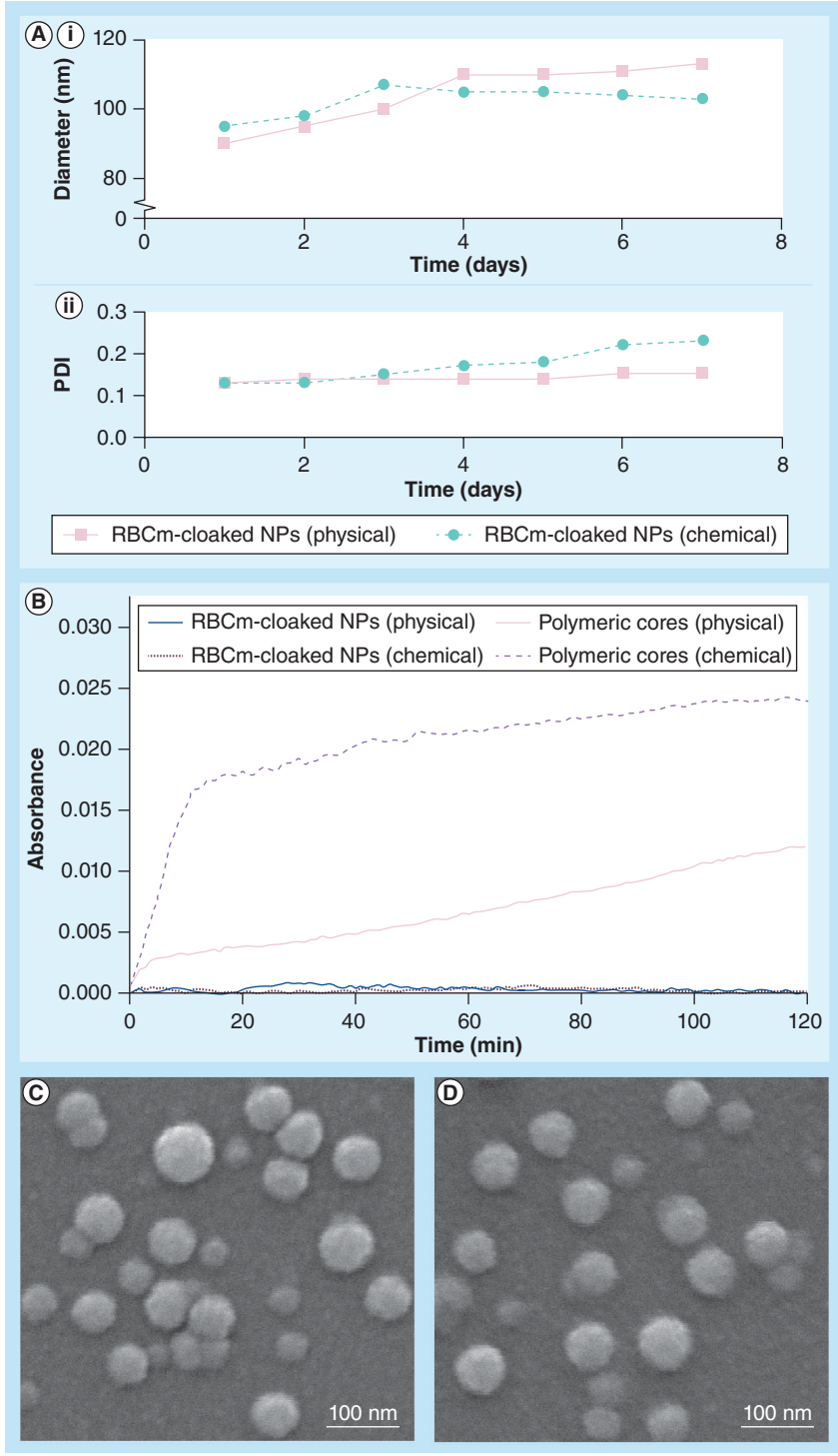

Figure 3. *In vitro* stability test and morphology of doxorubicin-loaded red blood cell membrane-cloaked nanoparticles. Doxorubicin (DOX) was loaded into the NPs through either chemical conjugation or physical encapsulation. **(A)** Long-term stability of DOX-loaded RBCm-cloaked NPs in terms of **(Ai)** particle size (diameter, nm) and **(Aii)** PDI in phosphate-buffered solution, monitored for a period of 7 days at room temperature. **(B)** Stability of DOX-loaded RBCm-cloaked NPs and bare NP cores (without RBCm cloak) in 100% fetal bovine serum was assessed by measuring the UV absorbance at the wavelength of 560 nm. **(C & D)** Representative scanning electron microscope images of DOX-loaded RBCm-cloaked NPs, of which the drugs were loaded through **(C)** chemical conjugation or **(D)** physical encapsulation.
NP: Nanoparticle; PDI: Polydispersity index; RBCm: Red blood cell membrane.

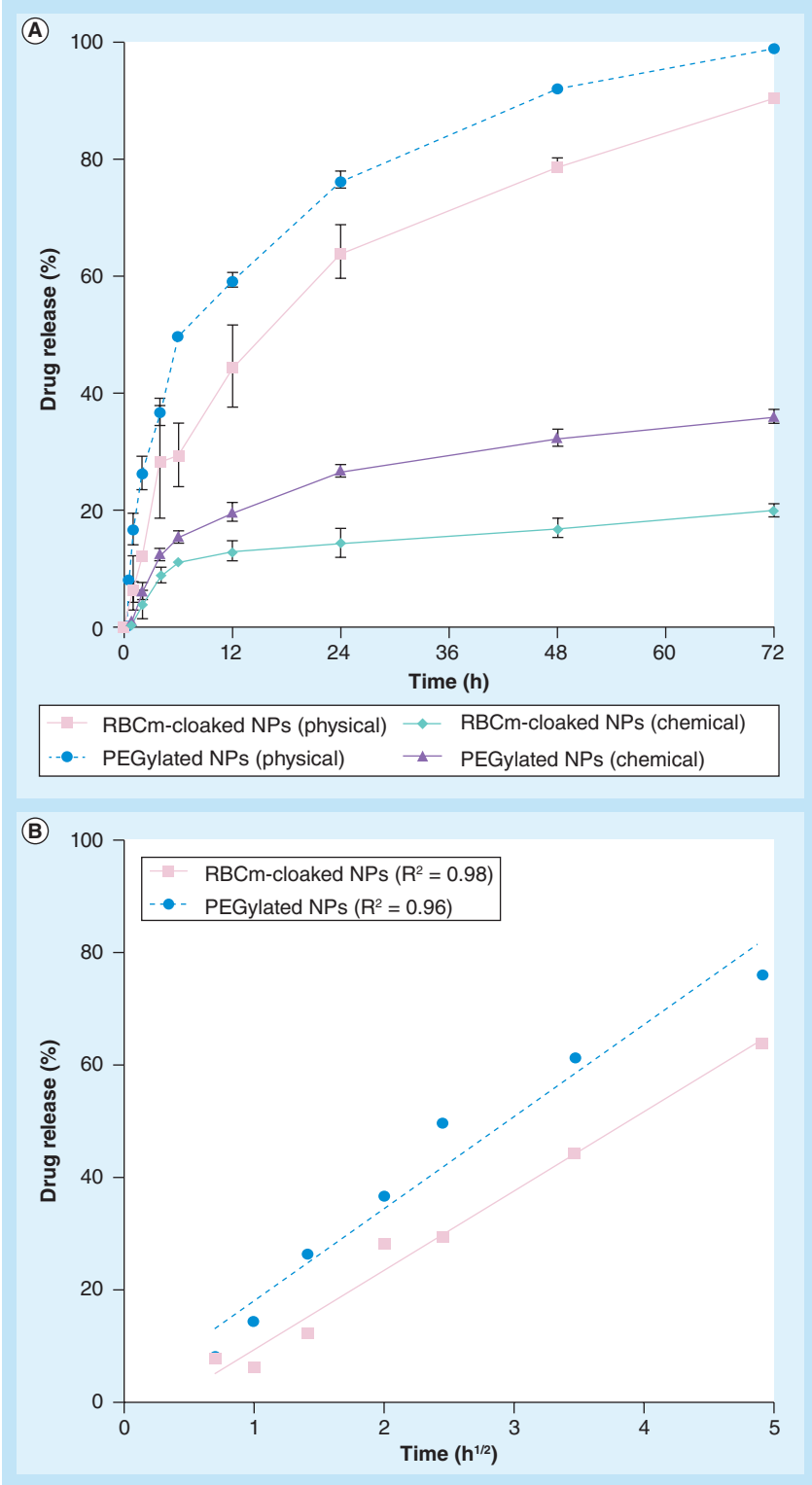

Figure 4. Drug release profiles and kinetics of the different doxorubicin-loaded nanoparticles. (A) Doxorubicin release profiles of RBCm-cloaked nanoparticles and PEG-coated nanoparticles. For these release studies, initial doxorubicin concentration inside the nanoparticles was 5 wt% for chemical conjugation and 1.8 wt% for physical encapsulation, respectively. **(B)** For the physical encapsulation systems, the drug release percentage was plotted against the square root of time, which yielded linear fittings using a diffusion-dominant Higuchi model.
NP: Nanoparticle; RBCm: Red blood cell membrane.

when formulations of chemical conjugation were examined, within the first 2 h only 5% of DOX molecules were released. Such difference has been attributed to the fact that covalent bonding of DOX molecules to the polymer backbone requires drug molecules to first be hydrolyzed from the polymer by bulk erosion before they can diffuse out of the polymeric matrix for release [11,12,16]. A more sustained-release profile resulted from drug–polymer covalent conjugation also suggests that chemical linkers responsive to environmental triggers can achieve better controlled drug releases when developing RBCm-cloaked NPs for advanced drug-delivery applications [13,17]. It is expected that acidic pH conditions will increase the drug-release rate of the polymeric cores because the pH drop will accelerate the degradation rate of the polymer backbone and facilitate the cleavage of the ester linkage between the drugs and the polymers [11].

In order to gain a better understanding of the role played by the RBCm cloak in drug retention, an established procedure for generating NPs by blending PLA–PEG diblock copolymers was followed to produce PEGylated NPs, where NP cores were coated and stabilized by a PEG layer instead of RBCm cloak [18]. It was hypothesized that if two formulations have similar NP cores, the difference in drug release will be primarily caused by the different abilities of the RBCm cloak and surface PEG coating in drug retention. By comparing DOX release from RBCm-cloaked NPs to that from PEGylated NPs, it was found that the release rate of the RBCm-cloaked NPs was lower; approximately 20% of DOX was released within the first 72 h in the RBCm-cloaked NPs, whereas 40% of DOX was released from the PEGylated NPs over the same time span. In fact, by using NPs formulated by PLGA–PEG diblock copolymers, surface PEG molecules have been found to hinder drug release from NP cores [19]. Hence, the observation that DOX is released at a higher rate from PEG-coated NPs compared with RBCm-cloaked NPs indicates that RBCm indeed acts as a diffusion barrier for DOX release. This observation is in accordance with previous studies demonstrating that phospholipid coating can act as a barrier to drug diffusion [20]. Such a role played by the RBCm cloak further suggests that strategies aimed at engineering lipid membrane coatings may allow for responsive drug releases from RBCm-cloaked NPs under certain environmental cues in addition to those achieved by chemical conjugations embedded in polymer cores [21].

To gain a quantitative understanding of the membrane-coating effect on drug retention, the drug-release profiles were analyzed using mathematical models established in previous particle drug-release studies. Since the degradation of PLGA polymer is markedly slower than the observed drug release for the physically loaded systems [22,23], the drug release kinetics can be solely attributed to diffusional drug efflux with negligible contributions from the polymer's hydrolysis. A diffusion-dominant Higuchi model was therefore applied to analyze the drug release profiles of RBCm-coated and PEGylated NPs with physically encapsulated DOX. Plotting the drug-release percentage against the square root of time yielded linear fittings with R^2 = 0.98 and 0.96 for the RBCm-cloaked and the PEGylated NPs, respectively (FIGURE 4B). The goodness of the fit implies a diffusion-controlled drug-release mechanism and further allows for the derivation of the diffusion coefficient through the following Higuchi EQUATIONS 1 & 2 [24,25]:

$$M_t = Kt^{1/2} \quad (1)$$

$$K = A(2C_{ini}DC_s)^{1/2} \quad (2)$$

Where M_t is drug release at time t in hours, K is the Higuchi constant, C_{ini} is the initial drug concentration, C_s is the drug solubility, A is the total surface area of the particles and D is the diffusion coefficient. Given the particle dimensions, the drug-loading yield, the solubility of DOX in water (1.18 g/l), and the drug-release data, the diffusion coefficients were determined to be 6.6×10^{-16} cm^2/s and 8.2×10^{-16} cm^2/s for the RBCm-clocked and PEGylated NPs, respectively, which is consistent with previously reported drug diffusivities from PLGA/PLA NPs [26]. In this study, the bilayered membrane coating reduced the drug diffusivity by 1.2-times. It is expected that this retardation effect by the RBCm cloak would likely vary with different particle sizes, polymer types and therapeutic cargo.

In analyzing the release kinetics of NPs with chemically conjugated drugs, applying zero-order-kinetic model, first-order-kinetic model, and the Higuchi model resulted in poor fittings, which indicated that the systems possessed complex release profiles that involved a combination of drug diffusion, polymer relaxation and drug–polymer conjugate hydrolysis. Precise modeling of the retardation effect imposed by the RBCm cloak on the chemically conjugated DOX is beyond the scope of this study. Nevertheless, as identical particle cores are present in both RBCm-cloaked and PEGylated NPs, herein, it is hypothesized that polymer matrix relaxation and hydrolytic cleavage of the linkage are not dominant factors contributing to the difference observed in DOX release profiles. Instead, the authors attribute the slower release rate of the RBCm-cloaked NPs to two diffusion-dominated components: the diffusion of water into the polymer matrix; and the diffusion of the cleaved drugs outward across the polymer matrix [27]. As the membrane coating was shown to decrease the drug diffusivity in the physical entrapment system, it likely affected both the influx of water and the efflux of cleaved drugs in the covalent conjugate system, thereby resulting in a more sustained drug-release profile.

Cytotoxicity of DOX-loaded RBCm-cloaked NPs

Finally, the therapeutic potential of the DOX-loaded RBCm-cloaked NPs against an AML Kasumi-1 cell line was examined. AML, an illness characterized by uncontrolled growth and accumulation of leukemia blasts in the bloodstream, was chosen as a disease target because of the long circulation lifetime of the RBCm-cloaked NPs in the blood stream and their sustained drug-release profiles. The current standard of care for AML is high-dose anthracyclines, which raises serious concerns for cardiac toxicity [28]. Long-circulating NPs releasing therapeutic compounds in a sustained manner offer the opportunity to reduce the required dosing and improve upon the treatment efficacy. RBCm-cloaked NPs, where DOX was either physically loaded or covalently conjugated, exhibited higher toxicity by comparison to free DOX over a 72-h incubation period (FIGURE 5). In a previous study, it was demonstrated that these RBCm-cloaked NPs can be taken up by cancer cells in a tissue culture and the NPs remain in an intact core–shell structure after cellular internalization [9]. Therefore, the observed enhancement in efficacy can be likely attributed to endocytic uptake of NPs, which enables a high payload of drugs to enter the intracellular region [29]. Several previous reports have shown enhanced cytotoxicity of DOX through NP-based delivery of DOX [30,31]. The free DOX, by contrast, relies on passive membrane diffusion for cellular entry, which is less efficient and susceptible to membrane-bound drug efflux pumps [32–34]. AML cells, including

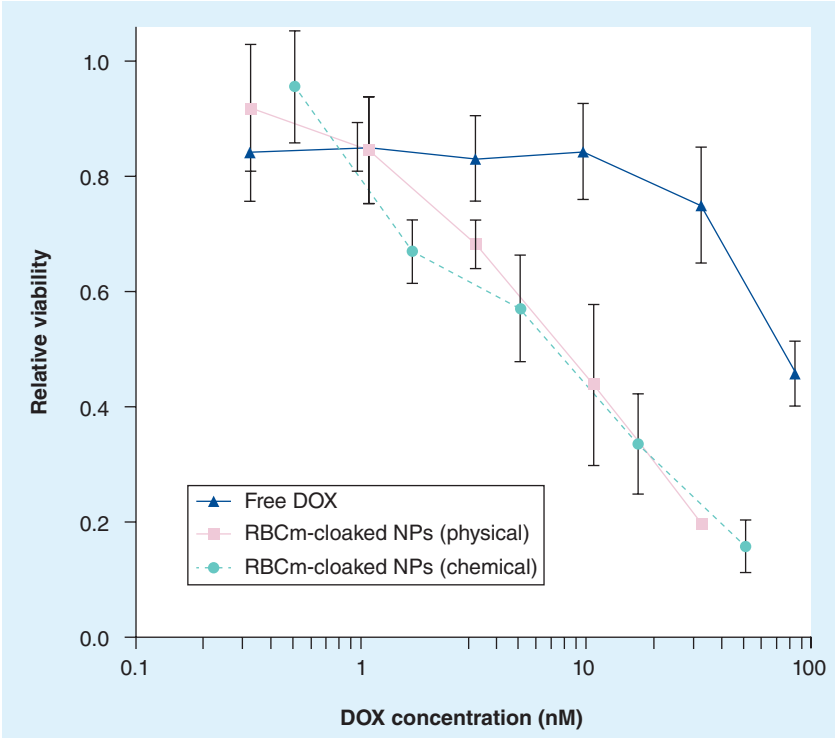

Figure 5. A comparative cytotoxicity study against the Kasumi-1 cell line established from the peripheral blood of an acute myeloid leukemia patient. Circles represent RBCm-cloaked NPs with chemically conjugated DOX, squares represent RBCm-cloaked NPs with physically encapsulated DOX and triangles represent free DOX. All samples were incubated with Kasumi-1 cells for 72 h prior to 3-(4,5-dimethylthiazol-2-yl)-2,5-diphenyltetrazolium bromide assay (n = 4).
DOX: Doxorubicin; NP: Nanoparticle; RBCm: Red blood cell membrane.

the Kasumi-1 cell line, are known to express membrane-bound drug efflux pumps, which decrease intracellular compartmentalization of DOX [35]. In particular, the Kasumi-1 cell line has been used previously as a P-glycoprotein-positive and anthracycline-resistant cell line in AML research [36,37]. The current study suggests that RBCm-cloaked NPs, with a prolonged circulation lifetime, sustained drug release and improved cell internalization, can become a promising platform toward the treatment of blood cancer. Further studies are warranted to investigate the therapeutic potential of these NPs *in vivo*.

Conclusion

In summary, herein, two strategies for loading drugs into an RBCm-cloaked NP delivery system were examined: physical encapsulation and chemical conjugation. Release studies suggest that the chemical conjugation strategy results in a more sustained drug-release profile. We further formulated PEGylated NPs that had the same NP cores but different surface coatings compared with RBCm-cloaked NPs. By comparing drug-release profiles of these two delivery systems, it was demonstrated that RBCm cloaks provide a barrier, slowing down the outward diffusion of encapsulated drug molecules. These results suggest that chemical modifications to the drug–polymer linkage in the NP core and engineering the NP surface coatings can both be explored to gain better control over drug releases of RBCm-cloaked NPs. In a following efficacy study by using the AML Kasumi-1 cell line, RBCm-cloaked NPs exhibited higher toxicity in comparison with free DOX. The previously observed long systemic circulation lifetime in the blood stream and the sustained drug-release kinetics reported in this study indicate that this biomimetic drug-delivery system may hold great promise for systemic delivery of payloads for the treatment of various diseases such as blood cancers. With further development, these RBCm-cloaked NPs are expected to become a robust drug-delivery system that combines the advantages of both synthetic polymers and natural cellular membranes.

Future perspective

RBCm-cloaked NPs represent a novel class of NP formulations bringing together both the long circulation lifetime of RBC, and the controlled drug retention and release of synthetic polymers. After gaining a deeper understanding of the roles played by the RBCm shell and the polymeric core, this NP formulation can be further tailored by engineering both parts to improve systemic delivery of therapeutic payloads. We believe that with continuing effort, this formulation will result in a robust delivery platform and make significant impact on both biomedical applications and nanotechnology research.

Financial & competing interests disclosure

This work was supported by the National Science Foundation Grants CMMI-1031239 and DMR-1216461. The authors have no other relevant affiliations or financial involvement with any organization or entity with a financial interest in or financial conflict with the subject matter or materials discussed in the manuscript apart from those disclosed.

No writing assistance was utilized in the production of this manuscript.

Ethical conduct of research

The authors state that they have obtained appropriate institutional review board approval or have followed the principles outlined in the Declaration of Helsinki for all human or animal experimental investigations.

Executive summary

Nanoparticle preparation

- To combine the advantages of a long circulation lifetime from red blood cells and controlled drug retention and releases from polymeric particles, red blood cell membrane (RBCm)-cloaked nanoparticles (NPs) were formulated in sub-100-nm sizes, containing:
  - Sub-100-nm polymeric cores made from doxorubicin (DOX)-poly(lactide acid) or poly(lactic-*co*-glycolic acid);
  - An erythrocyte exterior made from RBCm with preserved membrane proteins.

Drug-loading efficiency

- Two distinct methods of loading DOX as a model drug to the RBCm-cloaked NPs were examined:
  - Physical encapsulation, resulting in loading yields ranging from 0.9 to 1.8 wt%;
  - Covalent conjugation, resulting in an approximate loading yield of 5 wt%.

NP stability

- By monitoring NP size and UV absorbance, it was found that RBCm-cloaked NPs had a superior stability when compared with bare polymeric cores without RBCm cloaks, implying that the RBCm cloak played a significant role in stabilizing NPs in biological solutions.

Sustained drug release

- Release studies demonstrated that the drug–polymer covalent conjugation approach has a more sustained release profile than physical encapsulation, suggesting that the chemical linkers responsive to environmental triggers could achieve better controlled drug releases when developing RBCm-cloaked NPs for advanced drug delivery applications.

Controlled drug release

- By comparing RBCm-cloaked NPs with PEG-coated NPs it was found that RBCms acted as a diffusion barrier for DOX release. This observation was consistent with our quantitative analysis using Higuchi equations. Therefore, strategies aimed at engineering lipid membrane coatings can also enable responsive drug releases from RBCm-cloaked NPs under certain environmental cues.

Enhanced cytotoxicity

- DOX-loaded RBCm-cloaked NPs enhanced the efficacy against acute myeloid leukemia Kasumi-1 cells when compared with free DOX. This enhancement in efficacy can probably be attributed to endocytic uptake of NPs, which enables a high payload of drugs to enter the intracellular region.

References

Papers of special note have been highlighted as:
- of interest

1 Davis ME, Chen Z, Shin DM. Nanoparticle therapeutics: an emerging treatment modality for cancer. *Nat. Rev. Drug Discov.* 7(9), 771–782 (2008).
- **Excellent review of recent advances in nanoparticle therapeutics.**

2 Petros RA, DeSimone JM. Strategies in the design of nanoparticles for therapeutic applications. *Nat. Rev. Drug Discov.* 9(8), 615–627 (2010).
- **Excellent review of recent advances in nanoparticle therapeutics.**

3 Peer D, Karp JM, Hong S, Farokhzad OC, Margalit R, Langer R. Nanocarriers as an emerging platform for cancer therapy. *Nat. Nanotechnol.* 2(12), 751–760 (2007).

4 Farokhzad OC, Langer R. Impact of nanotechnology on drug delivery. *ACS Nano* 3(1), 16–20 (2009).
- **Excellent review on both challenges and opportunities in the emerging field of nanoparticle therapeutics.**

5 Alexis F, Pridgen E, Molnar LK, Farokhzad OC. Factors affecting the clearance and biodistribution of polymeric nanoparticles. *Mol. Pharm.* 5(4), 505–515 (2008).

6 Knop K, Hoogenboom R, Fischer D, Schubert US. Poly(ethylene glycol) in drug delivery: pros and cons as well as potential alternatives. *Angew. Chem. Int. Ed. Engl.* 49(36), 6288–6308 (2010).

7 Geng Y, Dalhaimer P, Cai S *et al.* Shape effects of filaments versus spherical particles in flow and drug delivery. *Nat. Nanotechnol.* 2(4), 249–255 (2007).

8 Yoo JW, Chambers E, Mitragotri S. Factors that control the circulation time of nanoparticles in blood: challenges, solutions and future prospects. *Curr. Pharm. Design* 16(21), 2298–2307 (2010).

9 Hu CM, Zhang L, Aryal S, Cheung C, Fang RH, Zhang L. Erythrocyte membrane-camouflaged polymeric nanoparticles as a biomimetic delivery platform. *Proc. Natl Acad. Sci. USA* 108(27), 10980–10985 (2011).
- **First report of the preparation and characterization of red blood cell membrane-cloaked nanoparticles as a new biomimetic drug delivery system.**

10 Dodge JT, Mitchell C, Hanahan DJ. The preparation and chemical characteristics of hemoglobin-free ghosts of human erythrocytes. *Arch. Biochem. Biophys.* 100, 119–130 (1963).

11 Aryal S, Hu CM, Zhang L. Polymeric nanoparticles with precise ratiometric control over drug loading for combination therapy. *Mol. Pharm.* 8(4), 1401–1407 (2011).

12 Tong R, Cheng J. Ring-opening polymerization-mediated controlled formulation of polylactide–drug nanoparticles. *J. Am. Chem. Soc.* 131(13), 4744–4754 (2009).
- **Excellent report of an elegant control over regioselectivity during the initiation step of synthesizing polymer–drug conjugates.**

13 Aryal S, Hu CM, Zhang L. Polymer–cisplatin conjugate nanoparticles for acid-responsive drug delivery. *ACS Nano* 4(1), 251–258 (2010).

14 Popielarski SR, Pun SH, Davis ME. A nanoparticle-based model delivery system to guide the rational design of gene delivery to the liver. 1. Synthesis and characterization. *Bioconjug. Chem.* 16(5), 1063–1070 (2005).

15 Fang RH, Aryal S, Hu CM, Zhang L. Quick synthesis of lipid–polymer hybrid nanoparticles with low polydispersity using a single-step sonication method. *Langmuir* 26(22), 16958–16962 (2010).

16 Tong R, Cheng J. Controlled synthesis of camptothecin–polylactide conjugates and nanoconjugates. *Bioconjug. Chem.* 21(1), 111–121 (2010).

17 Gao W, Chan JM, Farokhzad OC. pH-responsive nanoparticles for drug delivery. *Mol. Pharm.* 7(6), 1913–1920 (2010).

18 Gu F, Zhang L, Teply BA *et al.* Precise engineering of targeted nanoparticles by using self-assembled biointegrated block copolymers. *Proc. Natl Acad. Sci. USA* 105(7), 2586–2591 (2008).

19 Takae S, Miyata K, Oba M *et al.* PEG-detachable polyplex micelles based on disulfide-linked block catiomers as bioresponsive nonviral gene vectors. *J. Am. Chem. Soc.* 130(18), 6001–6009 (2008).

20 Zhang L, Chan JM, Gu FX *et al.* Self-assembled lipid–polymer hybrid nanoparticles: a robust drug delivery platform. *ACS Nano* 2(8), 1696–1702 (2008).

21 Pornpattananangkul D, Zhang L, Olson S *et al.* Bacterial toxin-triggered drug release from gold nanoparticle-stabilized liposomes for the treatment of bacterial infection. *J. Am. Chem. Soc.* 133(11), 4132–4139 (2011).

22 Avgoustakis K, Beletsi A, Panagi Z, Klepetsanis P, Karydas AG, Ithakissios DS. PLGA–mPEG nanoparticles of cisplatin: *in vitro* nanoparticle degradation, *in vitro* drug release and *in vivo* drug residence in blood properties. *J. Control. Release* 79(1–3), 123–135 (2002).

23 Li J, Jiang G, Ding F. The effect of pH on the polymer degradation and drug release from PLGA–mPEG microparticles. *J. Appl. Polym. Sci.* 109(1), 475–482 (2008).

24 Higuchi T. Rate of release of medicaments from ointment bases containing drugs in suspension. *J. Pharm. Sci.* 50, 874–875 (1961).

25 Siepmann J, Peppas NA. Higuchi equation: derivation, applications, use and misuse. *Int. J. Pharm.* 418(1), 6–12 (2011).

26 Budhian A, Siegel SJ, Winey KI. Controlling the *in vitro* release profiles for a system of haloperidol-loaded PLGA nanoparticles. *Int. J. Pharm.* 346(1–2), 151–159 (2008).

27 Pitt CG, Schindler A. The kinetics of drug cleavage and release from matrices containing covalent polymer–drug conjugates. *J. Control. Release* 33(3), 391–395 (1995).

28 Lowenberg B, Ossenkoppele GJ, van Putten W *et al.* High-dose daunorubicin in older patients with acute myeloid leukemia. *N. Engl. J. Med.* 361(13), 1235–1248 (2009).

29 Hu C-MJ, Zhang L. Therapeutic nanoparticles to combat cancer drug resistance. *Curr. Drug Metab.* 10(8), 836–841 (2009).

30 Ayen WY, Garkhal K, Kumar N. Doxorubicin-loaded (PEG)3–PLA nanopolymersomes: effect of solvents and process parameters on formulation development and *in vitro* study. *Mol. Pharm.* 8(2), 466–478 (2011).

31 Yoo HS, Park TG. Folate-receptor-targeted delivery of doxorubicin nano–aggregates stabilized by doxorubicin–PEG–folate conjugate. *J. Control. Release* 100(2), 247–256 (2004).

32 Huwyler J, Cerletti A, Fricker G, Eberle AN, Drewe J. By-passing of P-glycoprotein using immunoliposomes. *J. Drug Target.* 10(1), 73–79 (2002).

33 Rapoport N, Marin A, Luo Y, Prestwich GD, Muniruzzaman M. Intracellular uptake and trafficking of pluronic micelles in drug-sensitive and MDR cells: effect on the intracellular drug localization. *J. Pharm. Sci.* 91(1), 157–170 (2002).

34 Sahoo SK, Labhasetwar V. Enhanced anti proliferative activity of transferrin-conjugated paclitaxel-loaded nanoparticles is mediated via sustained intracellular drug retention. *Mol. Pharm.* 2(5), 373–383 (2005).

35 Dordal MS, Jackson-Stone M, Ho AC, Winter JN, Atkinson AJ. Decreased intracellular compartmentalization of doxorubicin in cell lines expressing P-glycoprotein. *J. Pharmacol. Exp. Ther.* 271(3), 1286–1290 (1994).

36 Mizutani M, Yamaguchi M, Miwa H *et al.* Frequent expression of *MDR1* and *MDR3* genes in acute myelocytic leukemia cells with t(8;21) (q22;q22). *Int. J. Oncol.* 10(3), 473–479 (1997).

37 Rao J, Xu Dr, Zheng Fm *et al.* Curcumin reduces expression of Bcl-2, leading to apoptosis in daunorubicin-insensitive $CD34^+$ acute myeloid leukemia cell lines and primary sorted $CD34^+$ acute myeloid leukemia cells. *J. Transl. Med.* 9, 71 (2011).